

Modification and Characterization of Aromatic Polyamide Reverse Osmosis membranes Doped TiO₂ Nanoparticles

M.H. El-Sayed, A.M. El-Aassar, M.M. Aboel-Fadl, M.A. El-Sheikh, M. M. Emara* and M.S. Abdel-Mottaleb**

Hydrogeochemistry Dept., Desert Research Center, El-Mataryia, *Chemistry Dept., Faculty of Science, Al-Azhar Univ. and **Chemistry Dept. Faculty of Science, Ain Shams Univ. Cairo, Egypt.

SYNTHESIS, characterization and reverse osmosis (RO) performance of modified polyamide (PA) membranes were studied. The modification includes acrylic acid (AAc) grafting and titanium dioxide (TiO₂) nano-particles doping using phase inversion method and chemically initiated procedure by benzoyl peroxide (BPO). The synthesized membranes elucidated good chemical stability with improved swelling behavior. XRD, mechanical properties, thermal stability and the surface morphology using atomic force microscope-tapping mode (AFM-TM) were studied.

RO performance of synthesized membranes was evaluated. The water flux increases by the increase of LiCl, AAc and TiO₂ concentration and applied pressure. While, the salt rejection (%) increases by the increase of AAc grafting (%), solvent evaporation and applied pressure. The synthesized PA-AAc-TiO₂ nano-composite membrane possesses good acceptable RO performance suitable for water desalination.

Keywords: Polyamide, Acrylic acid, TiO₂ nanoparticles, Characterization, Reverse osmosis membranes, Water desalination.

Although, water is nature's gift, it has attracted considerable attention during the last decades owing to serious shortage felt in many parts of the world. With the advent of rapid industrialization, cultivation and growing population, the water is becoming insufficient. Even though, attempts have been made for fuller utilization of the available natural water resources and it becomes necessary to adopt different desalination techniques to convert saline water resources into good water quality; Hegazy *et al.*⁽¹⁾. Reverse osmosis (RO) by polymeric membranes is considered as the simplest and most efficient technique for water desalination purposes; Rao *et al.*⁽²⁾ and Abu Tarboush *et al.*⁽³⁾. Two factors must be balanced for a reverse osmosis membrane to work properly, flux and salt

*corresponding Author, Tel. fax: (202)26389069;
E-mail: hameed_m50@yahoo.com

rejection (%). Both flux and salt rejection are dependent on membrane properties, solution chemistry, and operating conditions. Also, the membrane must also be resistant to compaction under pressure, and to chemical and biological degradation.

Many trials are introduced to prepare and modify the membrane such as the membrane grafting with hydrophilic monomers to increase the membrane hydrophilicity. The grafting can be carried out by different techniques including; chemical, radiation, photochemical and plasma-induced techniques. In these techniques, free radicals are produced and transfer to the substrate to react with monomer forming the graft co-polymers; Bhattacharya and Misra⁽⁴⁾.

Also, nano-particles have been used, as additives into reverse osmosis membrane, in order to increase their efficiency and reduce the cost of operation. Among many nanocomposite precursors, TiO₂ nanoparticles are increasingly being investigated because it is non-toxic, chemically inert, and low cost. TiO₂ has been extensively utilized in recent years to improve the permeability and antifouling properties of membranes due to photo-catalytic and super hydrophilicity effects; Madaeni and Ghaemi⁽⁵⁾. The trials to immobilize TiO₂ nanoparticles on flat polymeric membranes can be accomplished through deposition of TiO₂ nano-particles on the membrane surface or entrapment of TiO₂ nanoparticles in a polymer matrix of membranes by the addition of nanoparticles to the casting solution; Bae and Tak⁽⁶⁾.

The aim of the present work is concerned with modification, characterization and evaluation of RO performance of some aromatic polyamide (PA) membranes. The modifications include; AAc grafting and immobilization of TiO₂ nanoparticles into the polymer matrix. The synthesis was carried out via the phase inversion method using chemical initiation technique. Characterization of the synthesized membranes was carried out by evaluating the chemical stability at different pH, swelling behaviour, mechanical properties (tensile strength, elongation %), thermal stability through thermo-gravimetric analysis (TGA), X ray diffraction (XRD), FT-IR spectroscopy and surface morphology change by atomic force microscope-tapping mode (AFM-TM). Also RO performance was examined through studying the effect of membrane characteristics, operation conditions and feed water characteristics.

Experimental

Materials

Poly (m-phenylene isophthalamide) (PMPIPA) and N, N-Dimethyl acetamide (DMAC) were supplied by Aldrich. Acrylic acid (AAc): purity 99.9% was used as received and purchased from Merck, Germany. Titanium dioxide nano-particle (TiO₂): a commercial form (P25, 80% anatase, 20% rutile, BET area 50m²/gm) was obtained from Degussa, sodium dodecyl sulfate (SDS) used as surfactant. The other chemicals such as solvents and inorganic salts were reagent grade and used without further purification.

Egypt. J. Text. Polym. Sci. Technol. **14**, No.2 (2010)

Methods of membrane preparation

Different membranes of un-grafted, AAc grafted and/or modified with TiO₂ nano-particles were synthesized. The polymer was dissolved by stirring with different concentrations using DMAc as a solvent and LiCl as inorganic additives until complete dissolving and formation of homogenous casting solution. For (PA-g-AAc) membranes; AAc was added to the casting solution and the chemical initiation process was used by BPO. The desired temperature and time of the reaction was 85°C for 120 min, respectively. For synthesis hybrid organic/inorganic nano-composite membrane (PA-g-AAc/TiO₂), TiO₂ nano-particles were firstly modified with sodium dodecyl sulfate (SDS) as surfactant to prevent any aggregation of nano-particles in the membrane matrix. TiO₂ nano-particles were added to 0.7 % SDS at adjusted pH 4 with nitric acid, then stirring for 6 hr, the modified TiO₂ was obtained by centrifuge, then dried at 60°C for 24 hr. Different concentrations of TiO₂ (0-10wt.%) were added before the chemical initiation process. After the initiation process, the solutions were casted on glass plates, and then allowed to dry to obtain the membranes. After obtaining the membranes, they were immersed in coagulation H₂O bath for about 12 hr at 25°C. After that, the membranes were washed in de-ionized water and dried completely in a vacuum system or kept in distilled water until characterization and application.

Membrane characterization

The swelling (%) was calculated as follows:

$$\text{Swelling \%} = (W_{\text{wet}} - W_{\text{dry}}) \times 100 / W_{\text{dry}}$$

Where W_{dry} and W_{wet} represent the weights of the dry and wet membranes, respectively.

Analysis by FTIR was carried out using Gensis Unicam FT-IR spectrophotometer. The dimensions of the window, to which the membrane was fixed, were 1.5x 3cm.

The X-ray diffraction (XRD) patterns of the membranes were measured with Philips Model PW 3710 X-ray diffraction instrument.

Also, the mechanical properties (tensile strength and elongation) of membranes were evaluated using an Instron (Model-1195, England) at National Center for Radiation Research and Technology, Atomic energy Authority, Egypt.

The thermal gravimetric analysis (TGA) was carried out by using Shimadzu TGA system of type TGA-30.

Atomic force microscopy was used to analyze the surface morphology and the roughness parameters of the synthesized membranes. The device was Multimode-V5, Veeco Instruments Nano-scope (UK). The AFM imaging was

performed using tapping-mode. The tapping mode was selected because it was appropriate for imaging the samples such as polymer that could be easily damaged by the tip. Scanning was performed in 0.3Hz scanning rate with 256 pixels per line scan. The images cover an area of 5µm x 5µm.

The concentration of titanium (Ti) was estimated using the standard additive method and measured using inductively coupled argon plasma ICAP (thermo 6500).

Reverse osmosis properties (salt rejection and permeate flux) of the synthesized membranes were measured by laboratory DDS reverse osmosis system, model LAB-M20, manufactured by Alfa Laval Comp., Denmark. The effective membrane areas range from 0.036 to 0.72 m² (0.018m² per membrane). The salt rejection percent (R_s %) was calculated as:

$$R_s\% = (C_f - C_p/C_f) \times 100$$

Where C_f and C_p are the concentrations of feed and permeate water (product), respectively. The water flux through a semi-permeable membrane is directly proportional to the pressure across the membrane and expressed as shown by Lonsdal *et al.*, 1965 formula⁽⁷⁾:

$$J_{H_2O} = A (\Delta P - \Delta \Pi)$$

Where; J_{H₂O} (water flux, gm/cm². sec.) is expressed in weight of the product (grams) per unit membrane area (cm²) during operation time in sec. A is water permeability constant (g/cm².sec.atm), whose value depends on membrane characteristics, ΔP is the differential pressure applied across the membrane and, ΔΠ is the osmotic differential pressure (atm.) applied across the membrane.

Results and Discussions

Membrane preparation

Different membrane types were prepared using phase inversion method with BPO as a chemical initiator. The obtained membranes were divided into three main groups according to their chemical composition as listed in Table 1.

TABLE 1. Chemical composition of different synthesized membranes.

Group	PA (wt. %)	AAc (wt. %)	BPO (wt. %)	TiO ₂ conc. (wt. %)	Reaction temp. (°C)	Reaction time (min.)
I PA	5-15	-	-	-	-	-
II PA-AAc	7	5-100	2.5-10	-	40-110	30-180
III PA-AAc-TiO ₂	7	20	5	1-10	80	120

Effect of polymer concentration

It is obvious that; the swelling % of the different membranes decreases with increasing polymer concentration, Fig.1. This can be explained on fact that the membranes with low polymer concentration have more porous structure and high swelling %. The polymer concentration 7 wt. % was selected in this study.

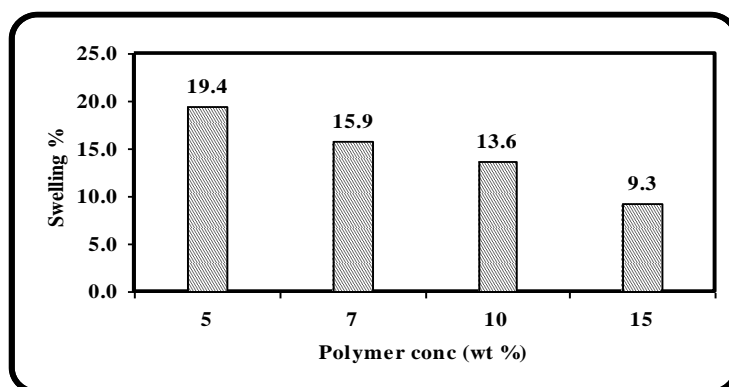


Fig.1. Effect of polymer concentration on the swelling % of aromatic PA membranes.

Effect of acrylic acid (AAc) concentration

AAc ($\text{CH}_2=\text{CH}-\text{COOH}$) monomer was grafted onto PA polymer backbone to incorporate new functional (COOH) groups and improve the hydrophilicity. The swelling % increases as AAc concentration increases up to certain limit (20 wt. %). Beyond this concentration, an abnormal decrease in the swelling % was observed, Fig.2. This may be due to the saturation of radical sites present on polyamide by chains growing progressively and high homopolymer formation (termination by recombination) in the reaction mixture. In other words, the presence of AAc in high concentration (more than 20 wt %) leads to the reaction of AAc monomer molecules with each other forming poly AAc homopolymer more than its reaction with the polymer chain to form co-polymer; Bhattacharya and Misra⁽⁴⁾ and Sun *et al.*⁽⁸⁾. However, AAc concentration not exceeds 20 wt. %.

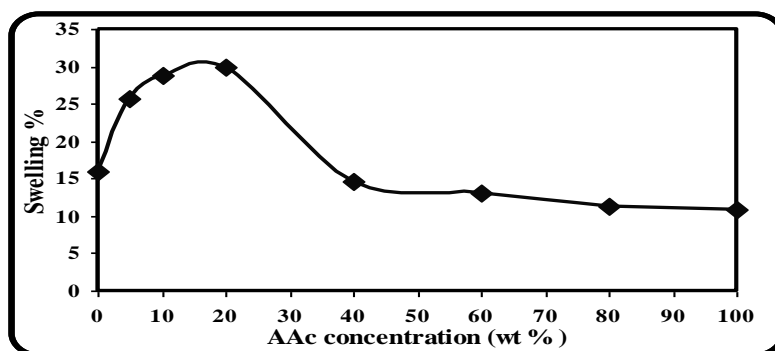


Fig. 2 . Effect of AAc monomer concentration on the swelling % of PA-g-AAc membrane.

Effect of initiator concentration

The increasing BPO concentration up to 5 wt % leads to significant enhancement in the swelling % of membrane, Fig.3. This can be explained based on that the increase of BPO concentration enhances the grafting process, indicated that the phenoxo primary free radical species ($\text{C}_6\text{H}_5\text{COO}^\bullet$), and/or the phenyl secondary free-radical species ($\text{C}_6\text{H}_5^\bullet$) formed by the dissociation of BPO in the polymer system. These radicals favor the formation of PA macro-radicals at the surface of polymer that participates directly in the initiation of grafting. Further increase decreased the swelling %, as a result of participation of the free radicals in a termination process; Patil and Fanta⁽⁹⁾. So the BPO concentration of 5 wt. % was selected.

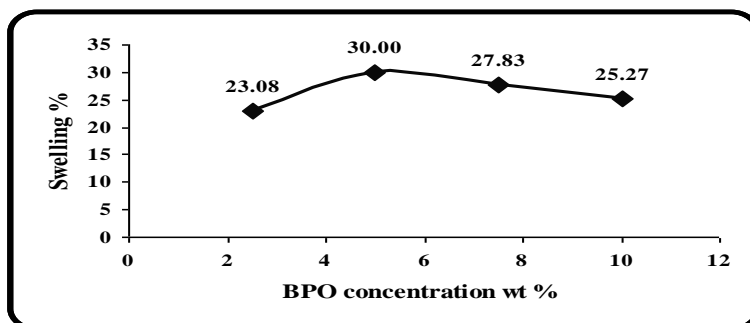


Fig. 3. Effect of benzoyl peroxide concentration on the swelling % of PA-g-AAc membrane.

Effect of reaction temperature

As shown in Fig. 4, increasing the reaction temperature up to 85°C increased the swelling %, due to the increase of the initiation and propagation rates of graft copolymerization, and the mobility of the reactive species. But beyond this temperature, the swelling % decreased, due to the increasing rate of homopolymerization reaction which resulted in a decrease in grafting rate and consequently swelling %; Sun *et al.*⁽⁸⁾.

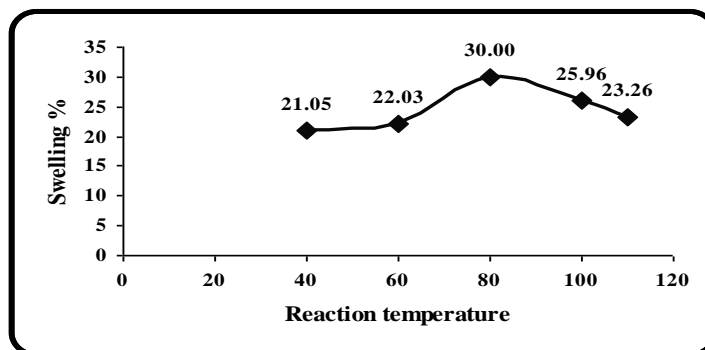


Fig. 4. Effect of reaction temperature on the swelling % of PA-g-AAc membrane.

Effect of overall reaction time

The grafting of PA with AAc was carried out at different reaction times in the range of 30-150 min., Fig. 5. By increasing the reaction time, up to 120 min., the swelling % increased, after that the swelling % slightly decreased.

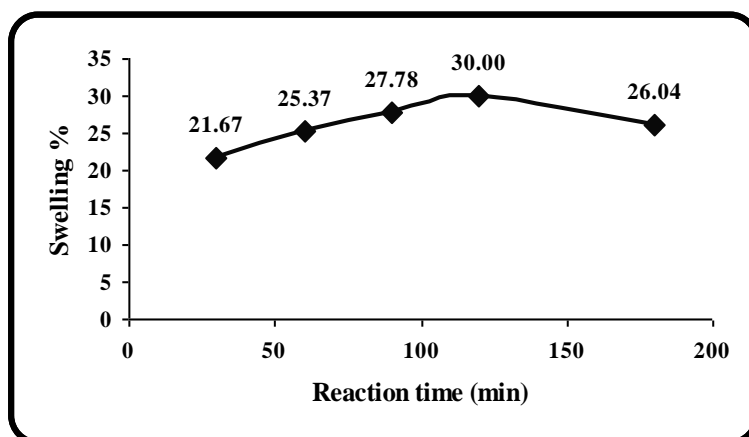


Fig. 5. Effect of reaction time on the swelling % of PA-g-AAc membrane.

Effect of TiO₂ concentration

Since TiO₂ has high affinity to water, the swelling % as well as the permeate flux can be improved; Cao *et al.*⁽¹⁰⁾. It has good compatibility with organic solvent (DMAc) which used in the preparation of PA casting solutions; Yang *et al.*⁽¹¹⁾. The grafting of PA with AAc had a positive effect in the synthesis of nano-composite membranes (PA-g-AAc/TiO₂), because the carboxylic groups of AAc act as coordination sites for the titania phase; Jeon *et al.*⁽¹²⁾. TiO₂ is actually connected to the membrane functional groups, so, the probability of the TiO₂ detached from the membrane matrix even under RO conditions is low as indicated by the chemical stability as mentioned after.

It is well known that if the surface of a mineral oxide (TiO₂) is exposed to water, it becomes hydrated, so the presence of water forms the hydroxyl layers Ti-OH groups on the particle surface; Velikovska and Mikulasek⁽¹³⁾. These OH groups lead to the increases of swelling % of the nano-composite membrane. As shown in Fig. 6, the swelling % increased from 30 % for neat PA-g-AAc to 37.3% with increasing TiO₂ concentration (up to 3 wt. % of polymer). This is because; the addition of a small amount of TiO₂ enhances the hydrophilicity and increases the number of micro-pores. Beyond this concentration, the swelling % decreased due to the high concentrations which lead to agglomeration of nano-particles in the polymer matrix, causing blocking of the micro-pores onto the membrane surface and decreasing the swelling %.

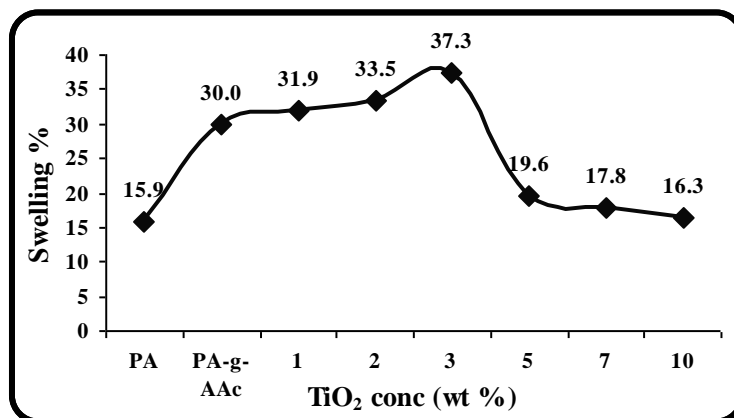


Fig.6. Effect of TiO₂ concentration on the swelling % of aromatic polyamide membranes.

Characterization of the synthesized PA membranes

Chemical stability of PA membranes

To elucidate the chemical stability of synthesized membranes, several pieces of the membranes were tested in different pH solutions ranging from 1 to 14 for 24 hr. The weight loss values are recorded to estimate the optimum pH for the operating system. Figure 7 shows that; the weight loss values do not exceed 4 % at pH 9. So, the aromatic polyamide can be used at wide range of pH values.

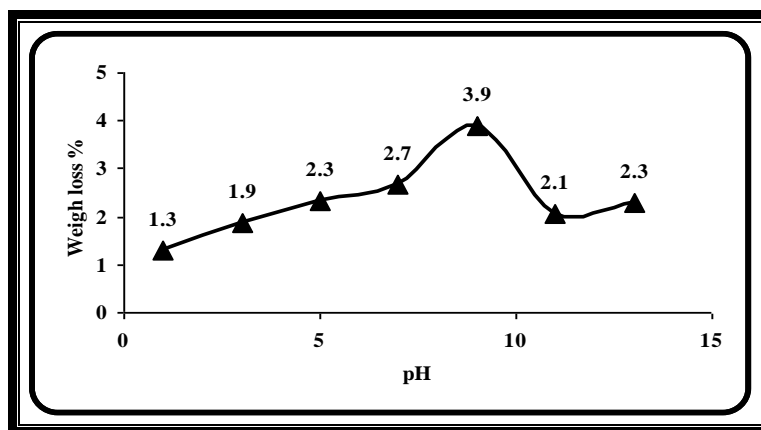


Fig. 7. Effect of pH on stability the aromatic PA membranes.

Also, The chemical stability of the TiO₂ nanoparticles were estimated by measuring the content of TiO₂ in different membranes either impregnated in distilled, acidic and alkali water or pressurized water under RO conditions for different times ranged from one to six days in case of impregnation and
Egypt. J. Text. Polym. Sci. Technol. **14**, No.2 (2010)

pressurized by RO unit. The concentration of Titanium (Ti) was estimated using ICAP (thermo 6500). All results indicate that; in case of the concentration of the nanoparticles (3 wt. %) there is no loss or TiO_2 nanoparticles release from the membrane matrix. These data confirm a presence of coordination and hydrogen bonding between the nanoparticles and polymer membrane matrix.

FT-IR spectroscopy

FT-IR spectroscopy was made to confirm the formation of graft copolymers and also to get some knowledge about their structures. Figure 8 shows the characteristic peaks of PA and PA-g-AAc membranes. Firstly; PA membrane exhibits number of peaks at $\sim 3453.88 \text{ cm}^{-1}$ which assigned N-H groups, the peak at 1620 cm^{-1} is characteristic to N-H (s) of amide, the peak at 1563 cm^{-1} is characteristic to C-N (s) of amide, and the peak at 1687 cm^{-1} is characteristic to C=O stretching vibration of the amide group.

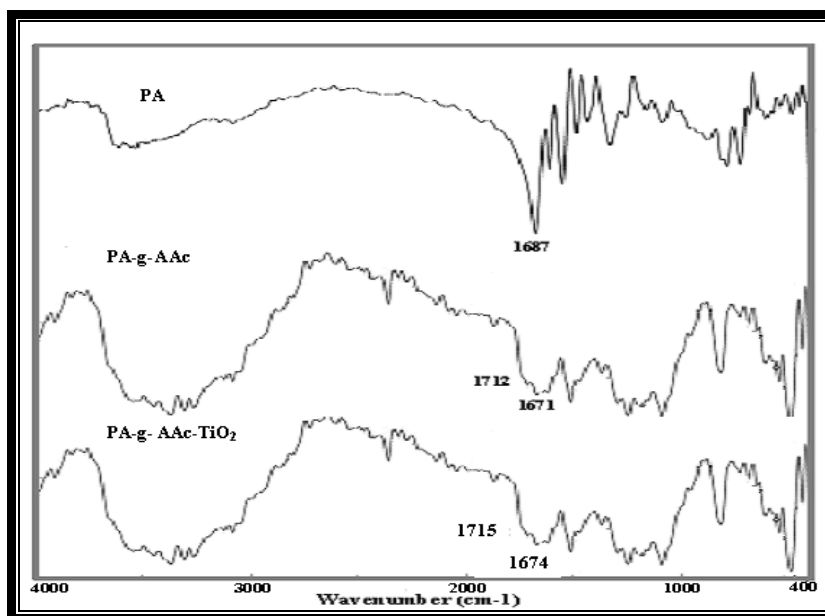


Fig. 8. FTIR spectra of synthesized PA, PA-g-AAc and PA-g-AAc/ TiO_2 nano-composite membranes.

With grafting of PA by AAc, the most noticeable changes of the spectra were as follow;

- The disappearance of the peak at 3453.88 cm^{-1} attributed to the N-H stretching vibrations (free) in the un-grafting polyamide implies that acrylic monomer was bonded to the membrane surface by replacing the hydrogen attached to the amide nitrogen.
- The appearance of a new peak at 1671.02 cm^{-1} is characteristic to N-R group, which confirms the formation of co-polymer chain (N- CH_2 -CH).

- The appearance of a new peak at 1712 cm^{-1} is characteristic to the carbonyl groups of AAc carboxylic groups.
- The new peak appears at 2991 cm^{-1} , corresponds to the stretching of OH bonds of AAc.

The existence of TiO_2 nanoparticles on the membrane surface shows no significant changes in spectra throughout wave numbers region. Probably, the non covalent band (coordination and hydrogen bonds) is formed between Titania and polymer chains; Mansourpanah *et al.*⁽¹⁴⁾.

X-Ray Diffraction measurements

As shown in Fig. 9 a, the curve of PA was broad without obvious peak features such broad peak which appears at $2\theta=24^\circ$ indicates the amorphous nature of aromatic PA, this finding is in agreement with previous work; Li *et al.*⁽¹⁵⁾. The broad peak on XRD is attributed to the average intersegment distance of the polymer chains. Figure (9 b) shows the effect of AAc grafting on PA, where there is no significant change in PA nature, but the change is strictly confined to the intensity of peaks. The intensity is significantly changed with AAc grafting; and its reduction is attributed to an increase in the intermolecular distance between the PA chains as a result of grafting; Saba and Mokhtar⁽¹⁶⁾. These results confirm that the AAc interact with the PA chains by replacing H-atom of the N-H group. The XRD results provide supporting evidence to the FTIR result that there is some specific chemical interaction between PA and AAc. Figure (9 c) shows the appearance of a new sharp peaks at $2\theta= 25, 27.5, 38^\circ$ are characteristic to TiO_2 nanoparticles (combined with the peaks of TiO_2 shown in Fig. (9 d), this in agreement with previous work of Kim *et al.*⁽¹⁷⁾. These results confirm the incorporation of TiO_2 nanoparticles with the polymer matrix.

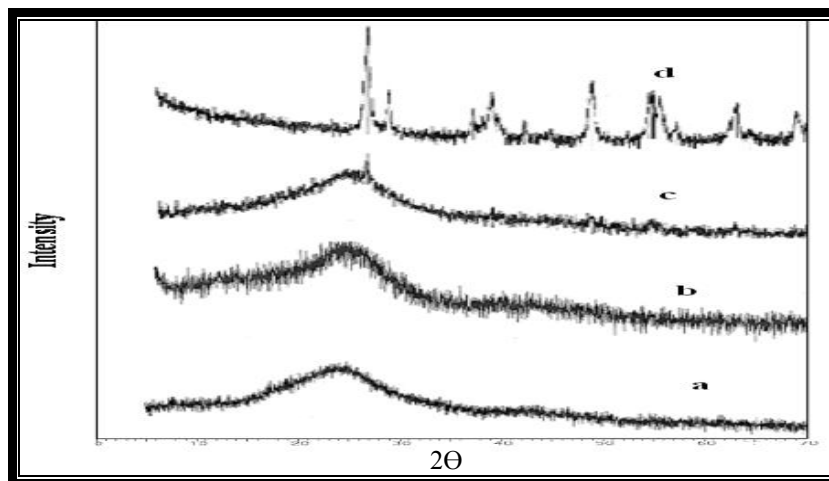


Fig. 9. X-ray diffraction pattern of a) Neat PA, b) PA-g-AAc (20%), c) PA-g-AAc/ TiO_2 nano-composite membranes and d) Degussa TiO_2 powder).

Mechanical properties

The mechanical properties include both tensile strength (MPa) and elongation (%) of different synthesized membranes are shown in Fig.10. The values of both tensile strength and elongation (%) at break increased from 45.26 to 53.8 (MPa) and from 8.36 to 21.2 (%) by 20% AAc grafting membrane, respectively. The increase of tensile strength is due to that the free COOH groups enhance the formation of hydrogen bonding leading to cross-linked network structure.

Also, the tensile strength values increase as TiO_2 concentration increases from 1 wt. % (53.8 Mpa) up to 5 wt. % (72.3 Mpa) then the tensile strength decreased. On the other hand, the elongation (%) at break decreased gradually with TiO_2 concentrations increase from 1 to 10 wt %. So, from the obtained results, it is suggested that only an appropriate amount (not exceed 3 wt. %) of TiO_2 could be used. These results indicate that when TiO_2 nanoparticles are incorporated into the polymer matrix in small concentrations, it arranged itself in the form of small particles. While the high concentrations lead to particles agglomeration and its distribution become less uniform which can cause brittleness of the membranes at high concentrations (10 wt. %); Zahoor *et al.*⁽¹⁸⁾.

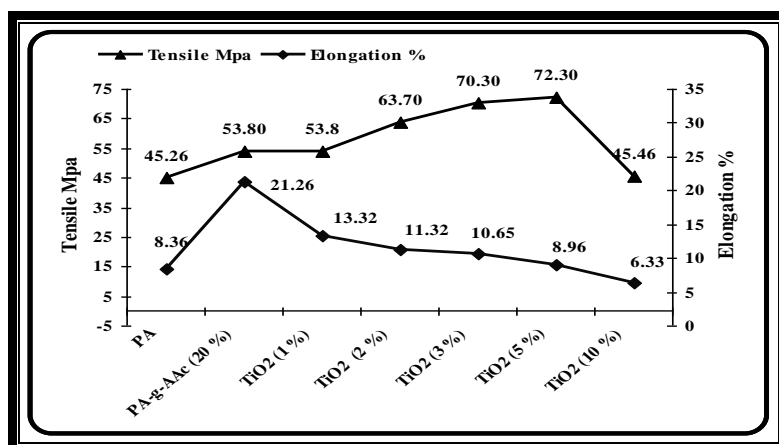


Fig. 10. The mechanical properties of different synthesized membranes.

Thermo-gravimetric analysis

The thermal decomposition patterns for all membranes are shown in Fig. 11. The synthesized polymeric membranes showed weight loss in three distinctive steps:

- During the first weight loss step, all the membranes exhibited relatively small losses of only about 1–5 % of their original weights. These weight losses were clearly attributable to evaporation of adsorbed moisture from the surfaces of the membranes.
- The second step showed considerable losses. However; this step represents the main thermal degradation step.

- The third step which occurred over 460, 370, and 450°C for PA, PA-g-AAc, and nano-composite PA-g-AAc/TiO₂, respectively, symbolizes the carbonization of the degraded products to ash.

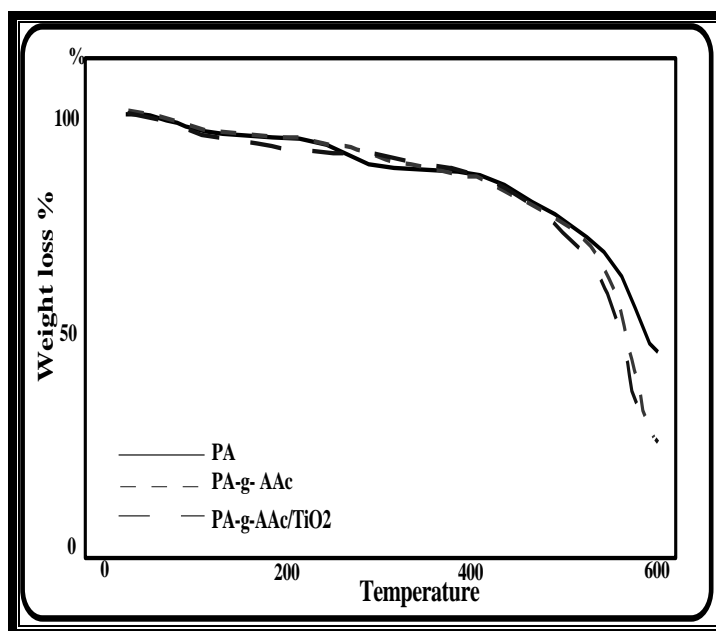


Fig.11. Thermo-gravimetric analysis of different synthesized membranes.

Generally; the thermal stability of aromatic PA membranes is decreased by AAc grafting due to the flexible connecting AAc groups to the PA chains. While it improved by TiO₂ doping due to the high thermal stability of the TiO₂ nanoparticles.

Atomic force microscopy (AFM)

AFM images of different membranes are displayed in Fig. 12. The roughness analysis parameters were chosen as key descriptors of membrane surface morphology: root-mean-square (rms) roughness (R_q), average roughness (R_a), and maximum roughness (R_m); Hoek *et al.*⁽¹⁹⁾.

The membrane surface roughness statistics for the three membranes considered in this study are listed in Table 2. The data indicate that R_q , R_a and R_m values increases in order PA-g-AAc/TiO₂ > PA-g-AAc (20 %) > PA.

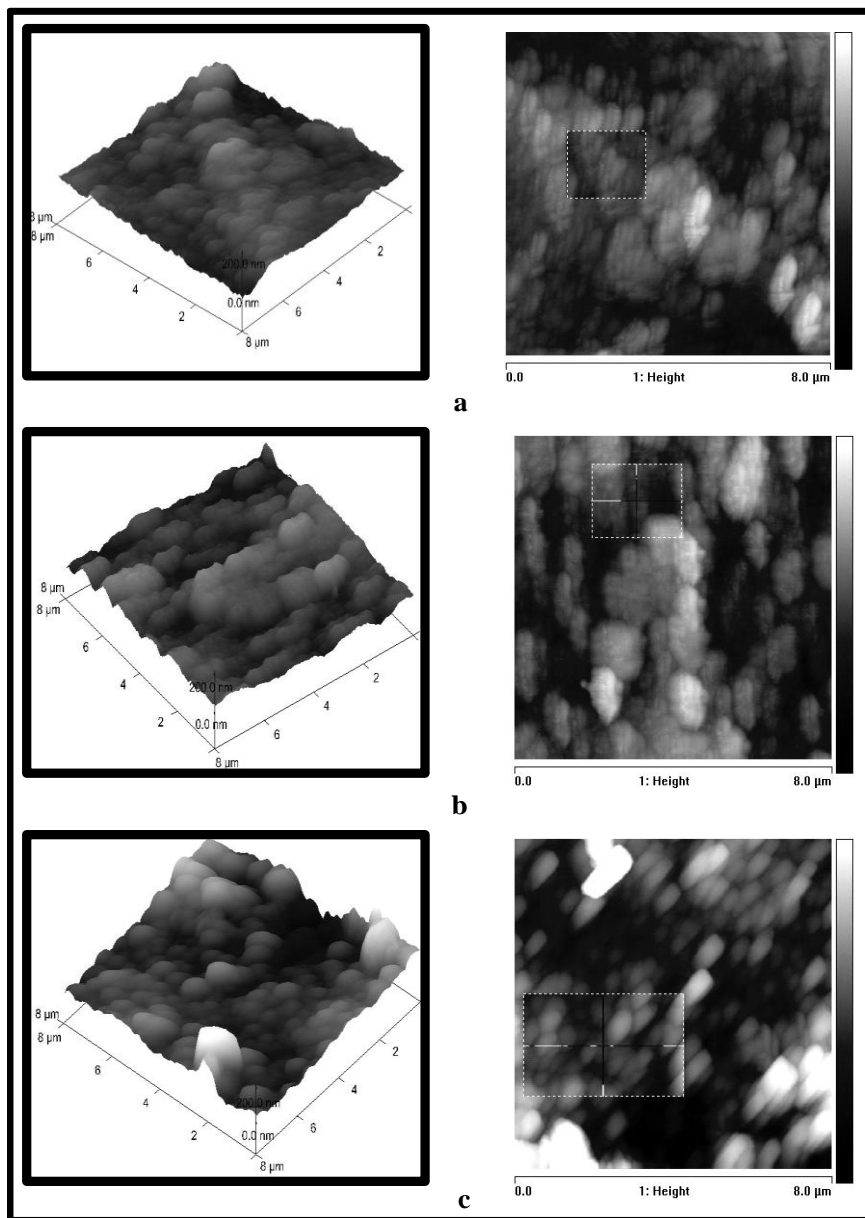


Fig. 12. AFM images showing the 3D (on the left side) and 2D (on the right side) of a) PA, b) PA-g-AAc (20%), and c) PA-g-AAc/TiO₂ (3 wt. %) membranes.

TABLE 2. Roughness parameters of different synthesized membranes .

Membrane	Roughness parameters (nm)		
	R_q	R_a	R_m
PA	21.3	17	140
PA-g-(20 wt.%)AAc	26.4	21.4	146
PA-g-(20 wt.%)AAc -(3 wt.%) TiO_2	45.9	33.5	343

From Table 2 and Fig. 12 (a, b), it could be seen, the un-grafted aromatic PA membrane appeared with homogenous morphology and distribution features. While the PA-g-AAc membrane showed more irregularities. Therefore, the roughness parameters of the grafted membrane increased compared to un-grafted membrane; Teng *et al.*⁽²⁰⁾. With TiO_2 doping (Fig. 12 c), the membrane surface is more rough than that of PA and PA-g-AAc membranes. This is related to appearance of nano-particles as nodular shapes (nodules are structural units observable at the membrane surface, Seung-Yeop and Kim⁽²¹⁾). It is thought that the increase of surface roughness of the nano-composite membrane also contributes to the increase of water flux. So, characterization of the synthesized membranes using AFM provides either AAc and/or TiO_2 into the aromatic PA membrane matrix. Also the difference in the roughness parameters from membrane to another can predict the improvement of RO performance (water flux). Since increase of surface roughness of the nano-composites membrane contributes to the increase of the water flux values; Lee *et al.*⁽²²⁾.

RO Performance of the synthesized membranes

To investigate the efficiency of different synthesized membranes in water desalination process, both water flux and salt rejection were measured after 8hr. at room temperature. The operation conditions included NaCl feed solution with 2000 ppm, applied pressure 30 bar, flow rate 5 l/min.

Several parameters are known to influence the salt rejection and water flux. These parameters include membrane characteristics, operation conditions and feed solution characteristics; Bartels *et al.*⁽²³⁾. The effect of these parameters on water flux and salt rejection are presented as follows:

Membrane characteristics

Effect of LiCl concentration : The effect of different LiCl concentrations (20-40 wt. % of polymer) on the membrane performance was studied, Fig. 13. It has been noted that; water flux increases with increasing LiCl concentration with slightly decrease in salt rejection (%). This is due to the increase of pores number on membrane surface leading to increase in water flux. On the other hand, the slight decrease in salt rejection was related to the diameter of lithium ion which is smaller than that of sodium and chloride ions, thus the diameter of the produced

pores by leaching of LiCl from the membrane matrix became smaller than sodium and chloride ions. Hence, the decrease in salt rejection % is very small; Mohamed and Al-Dossary⁽²⁴⁾.

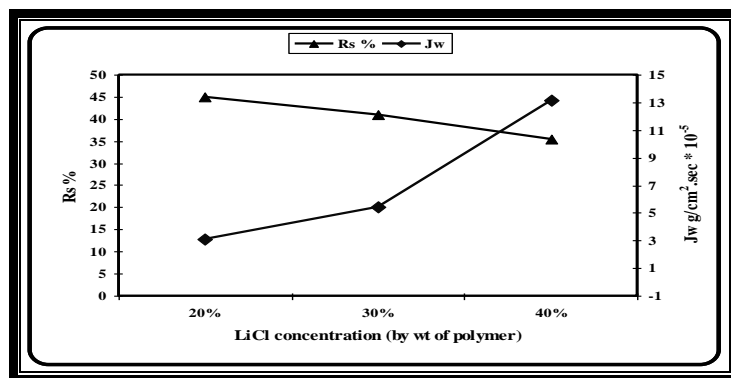


Fig. 13. Effect of LiCl concentration on RO performance of membranes.

Effect of acrylic acid (AAc) concentration

Increasing AAc grafting, *i.e.*, increasing the hydrophilic groups, surprisingly results in an increase of both water flux and salt rejection in the range of studied grafting (%), Fig. 14. This result can be explained according to the Donnan potential effect where a higher Donnan potential (higher -COO- groups on membrane surface) leads to an increase in overall salt rejection of the membrane; Bartels *et al.*⁽²³⁾. On the other hand, the water flux increases with increasing the grafting % reaching maximum value $15.5 \text{ g/cm}^2\cdot\text{sec} \times 10^{-5}$ using 20% AAc grafting, this can be explained on basis of AAc form hydrophilic anionic groups on the membrane surface, so the hydrophilicity of the membrane is enhanced thereby enhancing the water flux. It is expected that at highest grafting (%), the salt rejection will be lower and water flux will increase. This is presumably due to the high porosity of the membrane at such ratios.

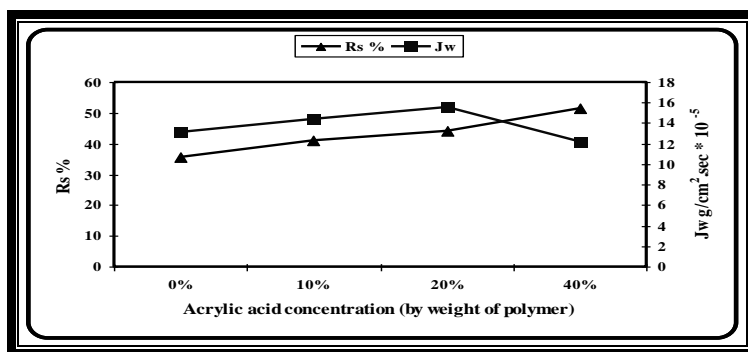


Fig. 14. Effect of AAc concentration on RO performance of membranes.

Effect of TiO_2 concentration

As shown in Fig. 15, the water flux of the membrane increases from 15.5 for PA-g-AAc to $\sim 34 \text{ g/cm}^2\cdot\text{sec} \times 10^{-5}$ with increasing the amount of TiO_2 up to 3wt.%, *i.e.* it improves the water flux with no significant change in salt rejection (%). This can be explained by two aspects; it renders the membrane more hydrophilic and also increases the surface roughness of membrane; Li *et al.*⁽²⁵⁾.

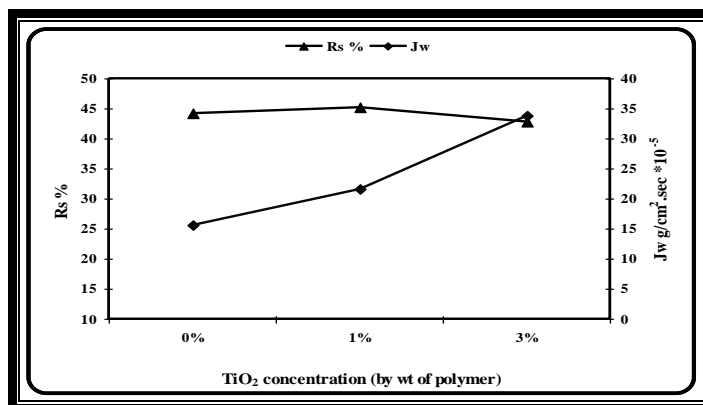


Fig. 15. Effect of TiO_2 concentration on RO performance of PA-g-AAc membrane.

Effect of solvent evaporation

It is well known in the membrane industry; the transport characteristic for a membrane can be controlled by adjusting the solvent evaporation temperature and oven exposure time; Joshi and Rao⁽²⁶⁾. Higher residual solvent levels result in a more open and porous matrix leading to increasing in water flux. Generally; during the solvent evaporation, the polymer concentration of top surface, which faces the air side, increases due to high loss of solvent causing low porosity of this surface. The other bottom surface which is in contact with the glass plate possesses more solvent due to the difference in diffusion rate of the solvent from this surface producing more porous side. As a result, an asymmetric flat sheet membrane is obtained which consists of thin dense skin surface layer supported on porous layer; Mohamed and Al-Dossary⁽²⁴⁾.

The effect of the solvent evaporation temperature on the RO properties of the synthetic membranes is shown in Fig. 16. With increasing the evaporation temperature from 60 to 85°C, the salt rejection increased from 38 to 49 %, while the water flux is decreased from 42 to 20 $\text{g/cm}^2\cdot\text{sec} \times 10^{-5}$.

Also, the effect of solvent evaporation time on both salt rejection (%) and water flux is shown in Fig. 17. The membrane was thermally treated at 70°C for various time intervals, ranges between 24 and 72 hr. The results show that an increase in salt rejection capability from 43 to 55 % and decrease in water flux from 34 to 8 $\text{g/cm}^2\cdot\text{sec} \times 10^{-5}$ as the solvent evaporation period increases from 24

to 72 hr. This can be attributed to the longer evaporation period at fixed temperature would result in lower residual solvent content with thicker skin layer of a membrane. This leads to a more dense structure and consequently improves the salt rejection of the membrane at lower water flux.

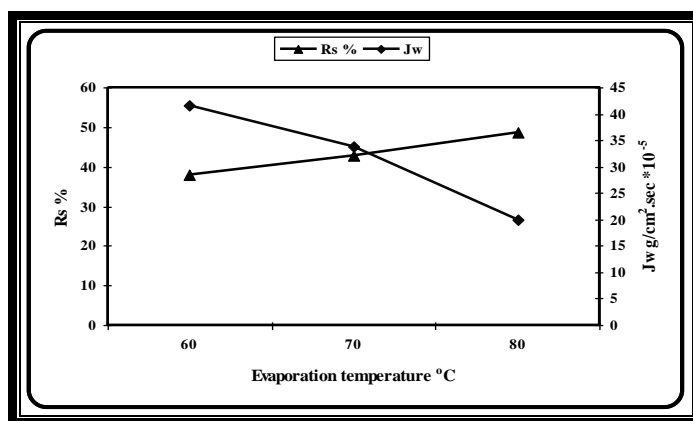


Fig. 16. Effect of evaporation temperature and time on RO performance of PA-g-AAc/ TiO₂ nano-composite membrane.

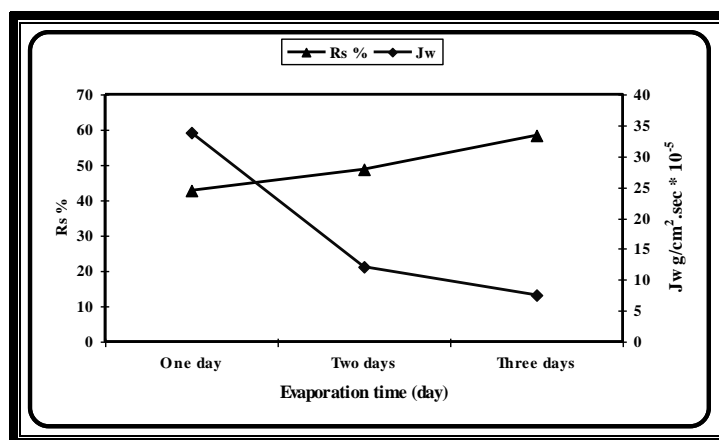


Fig. 17. Effect of evaporation time on RO performance of PA-g-AAc/ TiO₂ nano-composite membrane.

Effect of operation conditions

Applied pressure : From Fig. 18, it can be seen that, increasing the applied pressure (up to 50 bar) increased the values of both water flux (from 22 to 47×10^{-5} g/cm².sec) and the salt rejection (%) from 37 to 44 % simultaneously. The analogy of high flux-high salt rejection can be explained on the fact that the product water flux is directly proportional to the net applied pressure, while the

solute diffusion is not affected by any change in applied pressure. However, an increase in water flux reduces the concentration of the solute in permeate, thereby significantly increases the salt rejection; Schaep *et al.*⁽²⁷⁾.

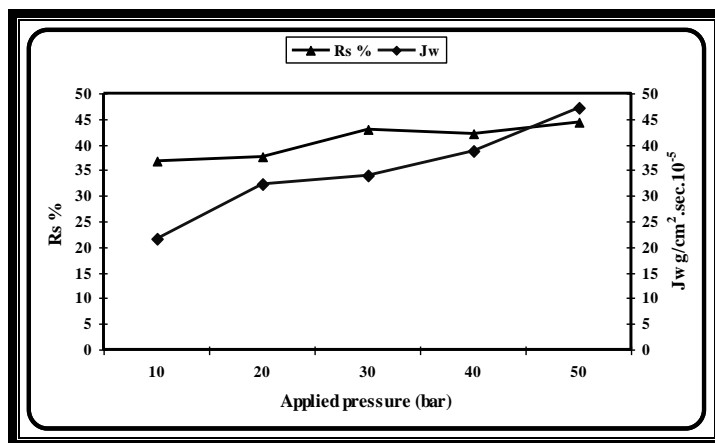


Fig. 18. Effect of applied pressure on RO performance of PA-g-AAc/ TiO₂ nano-composite membrane.

Effect of operation time

The influence of operation time on both water flux and salt rejection % up to 24 hr. using brackish water sample (TDS=3333 mg/l), (Fig. 19). It can be seen that the salt rejection (%) increased from 49 to 70%, while the water flux decreased from 13 to 10 ×10⁻⁵ gm/cm².sec with increasing the operation time from 8 to 24 hr. This is due to the increasing of salts accumulation in the pores of the membrane which reduces the water flux and increases the salt rejection.

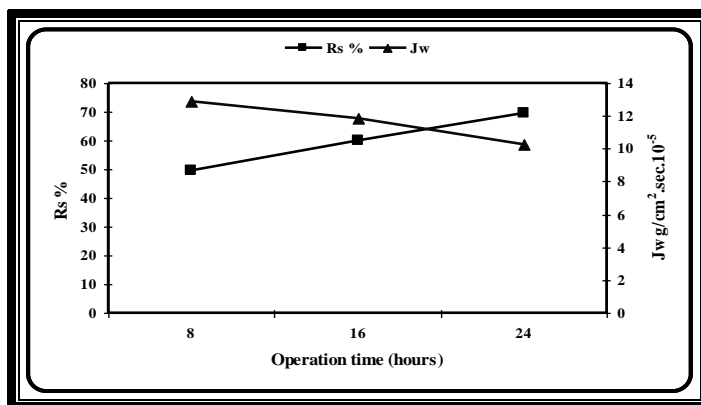


Fig. 19. Effect of operation time on RO performance of PA-g-AAc/ TiO₂ nano-composite membrane.

Effect of feed concentration

Reverse osmosis properties were investigated at different salinity values (2000 to 40000 μ mhos) feed solutions at the same operation conditions, *i.e.*, operation time (8 hr) and applied pressure of (30 bar), Fig. 20. It is obvious that, both water flux and salt rejection decrease with the increase of the feed concentration. The decrease of water flux with increasing the feed concentration can be explained as, the water flux through the membrane is proportional to the effective pressure (P_{eff}), *i.e.* $J_w \propto P_{\text{eff}}$ and $P_{\text{eff}} \propto P - \Delta\Pi$ where P_{eff} and P are the effective and applied pressures, $\Delta\Pi$ is the osmotic pressure. The increase of feed concentration at constant applied pressure leads to an increase in its osmotic pressure, which leads to a decrease in the effective pressure and a decrease in water flux. On the other hand, the decrease in salt rejection (%) by increasing the feed concentration can be explained by the effect of Donnan potential, Bartels *et al.*⁽²³⁾.

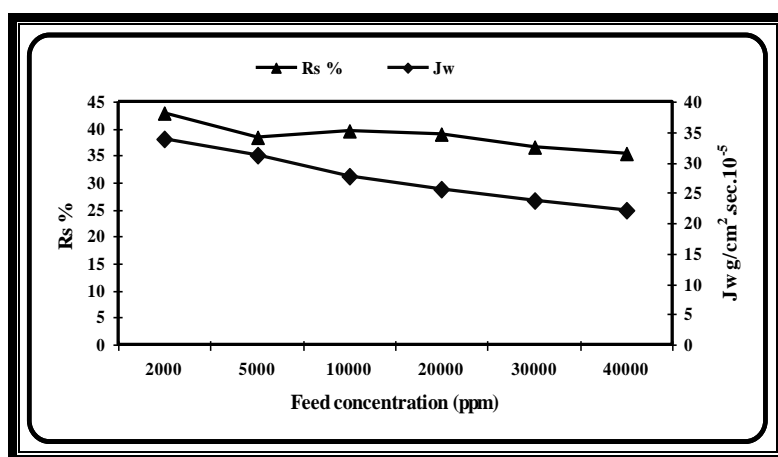


Fig. 20. Effect of feed concentration on reverse osmosis performance of PA-g-AAc/TiO₂ nano-composite membrane.

Conclusion

The present work concerned characterization and reverse osmosis performance of modified PA membranes. The modification includes the AAc grafting and TiO₂ nano-particles doping. Phase inversion method with chemically initiated procedure was used in the membrane modification. The effects of polymer concentration, monomer concentration, initiator concentration, time and temperature reaction and TiO₂ concentration on the obtained membrane properties were studied. The optimum conditions were investigated and included polymer concentration 7 wt.%, AAc concentration not exceeds 20 wt. %, BPO concentration 5 wt. % of monomer, and TiO₂ concentration 3 wt. %.

The modified membranes elucidated good chemical stability with weight loss value not exceeds 4% (at pH 9) and there is no any loss of nano-particles. The

synthesized membranes were characterized by studying the swelling behavior, XRD, FTIR and surface morphology using AFM.

The efficiency of the synthesized membranes for desalination process was evaluated (using NaCl solutions) by studying the effects of different parameters on both water flux and salt rejection (%). The different parameters include; membrane characteristics (LiCl concentration, AAc concentration, TiO₂ concentration, temperature and time of solvent evaporation), operation conditions (applied pressure, operation time) and feed solution characteristics (feed concentration). The obtained results show that the water flux increases with the increase of LiCl concentration, AAc grafting (%), TiO₂ concentration, applied pressure. While the salt rejection (%) increases by increasing AAc grafting (%), solvent evaporation temperature and time, applied pressure (up to 50 bar). PA-AAc-TiO₂ membrane possesses good acceptable RO performance and can be considered suitable for water desalination.

References

1. Hegazy, E.A., El-Assy, B.N., Dessouki, M.A. and Shaker, M.M., *Radiat. Phys. Chem.* **33**, 13 (1989).
2. Rao, A.P., Desai, N.V. and Rangarajan, R., *J. of Membrane Sci.* **124**, 263 (1997).
3. Abu Tarboush, B.J., Rana, D., Matsuura, T., Arafat, H.A. and Narbaitz, R.M., *J. of Membranes Sci.* **325**, 166 (2008).
4. Bhattacharya, A. and Misra, B.N., *Progress in polymer Science*, **29**, 767 (2004).
5. Madaeni, S.S. and Ghaemi, N., *J. Membrane Sci.* **303**, 221 (2007).
6. Bae, T. and Tak, T., *J. of Membrane Science*, **275**, 1 (2006).
7. Lonsdal, H.K., Merten, V. and Riley, R. L., *J. Appl. Polym. Sci.*, **9**, 1341-1362 (1965).
8. Sun, T., Liu, P. X., Xue, J. and Xie, W., *Eur. Polymer. J.*, **39**, 189-192 (2003).
9. Patil, D.R. and Fanta, G. F., *J. Appl. Polym. Sci.* **47**, 1765 (1993).
10. Cao, X., Ma, J., Shi, X. and Ren, Z., *Applied Surface Sci.* **253**, 2003 (2006).
11. Yang, Y., Wang, P. and Zheng, Q., *J. Poly. Sci. Part B: Polymer Physics*, **44**, 879–887 (2006).
12. Jeon, J.D., Kim, M.J. and Kwak, S.Y., *J. Power Sources*. **162**, 1304 (2006).
13. Velikovska, P. and Mikulasek, P., *Separation and Purification Technology*. **58**, 295 (2007).

14. Mansourpanah, Y., Madaeni, S.S., Rahimpour, A., Farhadian, A. and Taheri, A.H., *J. Membrane Sci.* **330**, 297 (2009).
15. Li, L., Zhang, S., Zhang, X. and Zheng, G., *J. Membrane. Sci.* **289**, 258–267 (2007).
16. Saba, M.W. and Mokhtar, S.M., *Polymer testing.* **21** , 337 (2002).
17. Kim, S.H., Kwak, S.Y., Sohn, B.H. and Park, T.H., *J. Membrane. Sci.* **211**, 157 (2003).
18. Zahoor, A., Sarwa, M. and Zulfiqar, S., *J. Sol-Gel Sci. Technol.* **44**, 41 (2007).
19. Hoek, E.M.V., Bhattacharjee, S. and Elimelech, M., *Langmuir* , **19** , 4836 (2003).
20. Teng, M.Y., Lee, K.R., Liaw, D.J., Lin, Y.S. and Lai, J.Y., *Eur. Polymer. J.* **36**, 663 (2000).
21. Seung–Yeop, K. and Kim, S.H., *Membrane. Environ. Sci. Techno.* **35** , 2388 (2001).
22. Lee, H.S., Im, S.J., Kim, J.H., Kim, H.J., Kim, J.P. and Min, B.R., *Desalination.* **219** , 48 (2008).
23. Bartels, C., Franks, R., Rybar, S., Schierach, M. and Wilf, M., *Desalination*, **184** , 185 (2005).
24. Mohamed, N.A. and Al-Dossary, A.O.H., *Eur. Polymer. J.* **39** , 739 (2003).
25. Li, J.F., Xu, Z.L., Yang, H., Yu, L. and Liu, M., *Applied Surface Sci.* **255** , 4725 (2009).
26. Joshi, S.V. and Rao, A.V., *Desalination*, **78** , 355-362 (1990).
27. Schaep, J., Vandecasteele, C., Peeters, B., Luyten, J., Dotremont, C. and Roels, D., *J. Membrane. Sci.* **163** , 229–237 (1999).

(Received 12/ 1/2011;
accepted 30/11/2011)

تحويل وتوصيف أغشية الضغط الاسموزي المنعكس من البولي أميد الاروماتي المطعم بحبيبات ثاني اكسيد التيتانيوم النانومترية

مجدى حسنى السيد ، عبد الحميد مصطفى الاعصر ، مصطفى محمد سعيد ، محمد السيد عبدالفتاح ، مصطفى محمود عماره* و محمد صبرى عبدالمطلب**
قسم الهيدروجيوكيمياء - مركز بحوث الصحراء - *قسم الكيمياء - كلية العلوم - جامعة الازهر و **قسم الكيمياء - كلية العلوم - جامعة عين شمس - القاهرة - مصر .

تناول البحث تحضير وتوصيف ودراسة كفاءة بعض أغشية الضغط الاسموزي المنعكس المستخدمه فى تحلية المياه والمحضرة من البولى أميد الاروماتي والمطعمة بحمض الاكريليك وثانى اكسيد التيتانيوم النانومتري. حيث تم تحضير تلك الاغشية بطريقة الصب والتجفيف مع استخدام البنزويل بيراكسيد كبادئ للتفاعل. تم تحديد انسب ظروف التحضير والتي اشتملت على تركيز البوليمر (٧ وزن %) ونسبة تطعيم حمض الاكريليك (٢٠ وزن % من البوليمر) وتركيز البنزويل بيراكسيد (٥ وزن % من البوليمر) وتركيز ثانى اكسيد التيتانيوم النانومتري (٣ وزن % من وزن البوليمر).

أوضحت دراسة خواص الاغشية المحضرة أنها تتميز بثبات كيميائي وأن فقد الوزن لايتعدى ٤% بعد ظروف التشغيل المختلفة. كما أظهرت النتائج زيادة نسبة الانتفاش من ١٥% للبولي اميد الاروماتي الى ٣٧,٣% للبولي أميد المطعم بكلا من حمض الأكريليك وثانى أكسيد التيتانيوم النانومتري. كذلك تم توصيف الأغشية المحضرة من خلال استخدام جهاز حيود الأشعة السينية ودراسة خواصها الميكانيكية وثباتها الحراري كما تم دراسة التغير فى طوبوغرافية سطح الأغشية باستخدام تقنية ميكروسكوب القوة الذرى مع قياس معاملات خشونة السطح المختلفة.

كذلك تم تقييم اداء ودراسة كفاءة تلك الأغشية المحضرة من خلال تقدير نسبة احتجاز الأملاح وكمية المياه المحلاة. حيث تبين أن كميته المياه المحلاة تزداد بزيادة تركيز كلوريد الليثيوم ونسبة تطعيم حمض الأكريليك وثانى أكسيد التيتانيوم النانومتري والضغط المستخدم. بينما تزداد نسبة احتجاز الأملاح بزيادة نسبة تطعيم حمض الأكريليك وزيادة حرارة وزمن التبخير والضغط المستخدم.

أظهر الغشاء المحضر من البولى أميد المطعم بكلا من حمض الأكريليك وثانى أكسيد التيتانيوم كفاءة فى تحلية المحاليل الملحية من كلوريد الصوديوم مما يعنى امكانية استخدامه فى تحلية مياه الابار المالحة ومياه البحر.